VOL.40 Nº3 2023
https://doi.org/10.22491/rmct.v40i3.11270.en

Impact testing to evaluate the toughness of ultra-high hardness steel for ballistic applications

Charles Hudson Martins de Vasconcelos[1,3], charles.vasconcellos@ime.eb.br, Orcid 0000-0002-3472-2998
Cristhian Ricardo Loayza Loayza[2], crislo@ufpa.br, Orcid 0000-0002-0662-715X
Ademir Ângelo Castro Filho[2], engangelo80@gmail.com, Orcid 0000-0003-4713-0817
Eduardo de Magalhães Braga[2], edbraga@ufpa.br, Orcid 0000-0003-0739-7592
Andersan dos Santos Paula[1], andersan@ime.eb.br, Orcid 0000-0002-0904-4240
Ricardo Pondé Weber[1], rpweber@ime.eb.br, Orcid 0000-0002-7431-8316
[1]Instituto Militar de Engenharia - IME, [2]Universidade Federal do Pará - UFPA,
[3]Centro de Instrução Almirante Braz de Aguiar - CIABA

ABSTRACT: *Ultra-high hardness armor grade steels are commonly used in sectors such as patrol vehicles, cash-in-transit vehicles, armored personnel carriers, building protection, among others. The aim of this work was to evaluate the toughness of a material in this class by determining the ductile-to-brittle transition temperature (DBTT) using some of its definitions. Charpy impact tests were conducted and the fracture faces of the specimens were evaluated through both macroscopic and microscopic analysis. The tests were conducted at temperatures ranging from -60°C to room temperature, using specimens extracted longitudinally to the rolling direction. Micrographic analyses indicated that determining the DBTT using the energy absorption criterion is appropriate and reliable. The obtained results show that, based on an absorbed energy of 12.92 J, the transition temperature is -27.73°C.*

KEYWORDS: *Toughness, ductile-to-brittle transition temperature, impact test, ultra-high hardness steel.*

RESUMO: Os aços de nível de blindagem de ultra-alta dureza são comumente utilizados nos setores de veículos de patrulha, veículos de transporte de valores, viaturas blindadas de transporte de pessoas, proteção de edificações, entre outros. O objetivo deste trabalho se constituiu na avaliação da tenacidade de um material dessa classe, determinando a temperatura de transição dúctil-frágil (TTDF) utilizando algumas das suas definições. Realizou-se ensaios de impacto Charpy e a avaliação combinada das faces de fratura dos corpos de prova por macroscopia e microscopia. Os testes foram realizados em temperaturas que variaram de -60°C a temperatura ambiente com corpos de prova retirados longitudinalmente à direção de laminação. As análises micrográficas ostentaram que a determinação da TTDF por critério de absorção de energia é adequada e confiável. Os resultados logrados são que, com base em 12,92 J de energia absorvida, a temperatura é -27,73°C.

PALAVRAS-CHAVE: Tenacidade, temperatura de transição dúctil-frágil, ensaio de impacto, aço de ultra-alta dureza.

1. Introduction

In recent decades, studies involving the field of armor have always been engaged in efforts to provide light armor technologies that can defeat projectiles (Armor-Piercing, AP). To meet these requirements, the availability of tempered and quenched armor steels has been increased, and most importantly, the MIL-DTL-46100E specification has been upgraded to High Hardness Armor (HHA) steels [1]. Although this metal specification has met the intended applications, considerable efforts have been made to develop ultra-high hardness—quenched and tempered (UHH-Q&T) steels with a hardness of 600 HB or more [2].

The various types of steel offered by each supplier are generally differentiated according to a specific and increasing hardness value. The lowest hardness value corresponds to rolled homogeneous armor steel (RHA – 380-430 HBW), then medium hard armor steel (MHA - 420-480 HBW), HHA steel (480-540 HBW), and the highest level of hardness is reached with UHA or UHH-Q&T steel (570-640 HBW) [3].

Focusing on the projectile-target interaction, it can be determined that penetration mechanisms result from the property that represents the degree of deformation a material can withstand before fracturing. In ductile materials, fracture occurs due to the initial stress wave, radial fracture, shattering, plugging, frontal petaling, rear petaling, fragmentation and ductile hole enlargement. However, when a brittle material is used, the entire study can be summarized by the characteristics of fragmentation [4].

These phenomena bring up the need to determine a limit temperature, below which the material's fracture behavior changes from ductile to brittle, in order to predict occurrences of brittle fracture. This temperature is called the Ductile-to-Brittle Transition Temperature (DBTT) of materials and the Charpy impact test is considered to be one of the most suitable for studying this issue [5-7].

By collecting energy absorption data through the Charpy impact test of metallic materials such as UHH-Q&T steel at various temperatures, the DBTT of this material can be determined. It is usually seen that there are two levels of absorbed energy, called the lower shelf and the upper shelf, and a region between them, called the transition zone [8-12].

It is therefore known that at temperatures corresponding to the lower energy absorption shelf, the material will fracture, mainly in a brittle manner with a predominance of the cleavage fracture micromechanism, while at temperatures corresponding to the upper energy absorption shelf, the material will fracture in a mostly ductile manner due to the coalescence of microcavities. A laborious task, however, is to determine the DBTT, which will be a reference temperature for the change in the material's fracture behavior from ductile to brittle as the temperature decreases [10, 13-15].

Checking how the fracture face looks is one of the methodologies for designating the DBTT, ranging from a fracture with a 100% shiny to 100% opaque appearance, and this characterization is done exclusively by visual observation of the fracture face, making it possible to establish a temperature at which the change in fracture micromechanism occurs. However, a suitable criterion would be needed to define the DBTT, as it would be difficult to determine this in experimental practice by evaluating these fractured specimens alone. For this purpose, the methodology indicated in ASTM E23 [16], which is the standard for carrying out the impact test, can be used.

However, the visual comparison method described in the standard is inaccurate, as the photographs to be used for comparison with the fracture faces of the test specimens leave something to be desired in terms of quality, resulting in a comparison with a high probability of inaccuracy [17-20]. It is therefore important to apply other methodologies to determine the DBTT. In the simplest and most accurate method, the DBTT is determined from the curve of absorbed energy as a function of temperature, and one possible criterion in this scenario is to consider that the DBTT is the temperature at which the average energy between the upper and lower levels of the curve is reached, illustrated in Fig. 1 [21-23].

In this context, the objective of this work was to determine the DBTT using some of its definitions combined with macroscopic and microscopic analyses of the fracture surface and metallurgical factors. Different test temperatures were used, in order to cover the range from temperatures at which the material of interest is expected to show 100% brittle fracture to temperatures at which 100% ductile fracture occurs.

2. Material and methods

2.1 Material

The material under study is UHH steel with a yield strength of 1500 MPa, thickness 5 mm, quenched and tempered (QT), classified as armor grade. This material meets the requirements for shape tolerances in accordance with EN 10029 [24], flatness tolerances in accordance with EN 10029 Class N – Steel Type L [24] and surface properties in accordance with EN 10163-2 Class B Subclass 3 [25].

The applicability of this material is as an additional protective sheet, or in cases where weight is critical, providing protection against both penetration and explosions. This same material is used in patrol vehicles, cash-in-transit vehicles (CIT), armored personnel carriers (APCs), building protection and other sectors. The chemical composition and mechanical properties of the material, specified in the standard, are shown in **Tables 1** and **2**, respectively.

Table 1 - Main chemical composition of the material (% mass).

C	Si	Mn	Ni	Cr	Mo	B	S	P
0.47	0.70	1.00	3.00	1.50	0.70	0.0005	0.003	0.01

Source: [26].

Table 2 - Main mechanical properties of the material.

Hardness HBW	Yield strength $Rp_{0.2}$ mín. MPa	Ultimate strength R_m min. MPa	Elongation %
570-640	1500	2000	7

Source: [26].

2.2 Sample preparation

The test specimens were extracted from a 500 x 500 x 5 mm plate of UHH-Q&T steel using the electrical discharge machining process. The specimen dimensions follow the sub-size classification of ASTM E23 [16], i.e., 10 x 5 x 55 mm, with a 2 mm deep V--notch in the 5 mm thickness, a 45° angle, and a root radius of 0.25 mm at the center of the specimen, verified using a profile projector and an optical microscope (OM)).

2.3 Charpy impact test

The Charpy impact tests were conducted in a Panambra impact tester, model PW30/15R, with a 30 J hammer, in accordance with ASTM E23 standard [16], using three specimens for each temperature. The tests began at room temperature (20.8°C) and were extended to lower temperatures: 0°C, -20°C, -40°C and -60°C. To reach these temperatures below room temperature, the specimens were inserted into liquid nitrogen, thus obtaining the absorbed energy as a function of temperature.

In order to evaluate the data obtained through the Charpy test, a curve of absorbed energy as a function of temperature is drawn up, but for better clarity in the analysis, this curve must be adjusted, and the method used was based on that proposed by Ericksonkirk, Shaikh and Ericksonkirk [27]. Using this method, the absorbed energy data as a function of the temperatures used in the test was adjusted using the formulation based on the hyperbolic tangent, which complies with Eq. 1.

$$Y = A + B * tanh \frac{T - D}{C} \qquad (1)$$

In Eq. 1, Y is the variable to be adjusted and T is the test temperature variable. The adjustment variables A, B, C and D are illustrated in **Fig. 1** and are defined as follows: A: average of the energies between the upper and lower shelves; B: range between the energies of the upper and lower shelves; C: half of the transition temperature range; and D: temperature of the average of the lower and upper shelves.

The DBTT value was established according to the following definitions:

- $DBTT_{EA}$: Ductile-to-Brittle Transition Temperature at which the arithmetic mean of the absorbed energies in the upper and lower shelves occurs.
- $DBTT_{BN}$: Ductile-to-Brittle Transition Temperature at which zero ductility transition occurs, i.e., 100% brittle fracture.
- $DBTT_{ND}$: Ductile-to-Brittle Transition Temperature at which there is zero brittleness transition, i.e. 100% ductile fracture.

Fig. 1 - Illustration of the adjustment variables of the hyperbolic tangent equation.

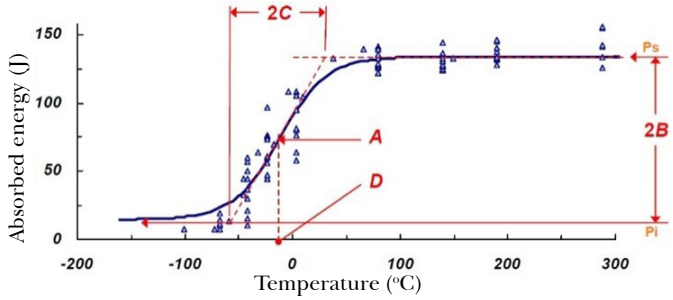

Source: [27].

2.4 Macroscopy versus microscopy of the fracture

Fracture surface analysis was conducted on specimens fractured in Charpy impact tests. The samples were previously cleaned in an ultrasound machine using an acetone solution. For imaging, a ZEISS SteREO Discovery V12 optical stereomicroscope and a FEI Quanta FEG 250 scanning electron microscope (SEM) were used, in accordance with ASTM standard E2142 [28].

3. Results and discussion

The microstructural aspect of the BM observed via OM, the presence of columnar laths and lath blocks after etching with 2% nital solution, can be seen in **Fig. 2(a)**, which confirms that the material is tempered martensitic steel. **Fig. 2(b)** shows the SEM image, which indicates that the laths shown in the previous image are acicular martensite laths.

One of the main purposes was to determine whether or not the material under study exhibits a ductile-to-brittle transition with decreasing temperature and, if so, in what temperature range the phenomenon occurs. The ductile-to-brittle transition is related to temperature by the impact energy measured in the test.

Fig. 2 - Microstructure of BM: (a) micrograph via OM; (b) micrograph via SEM.

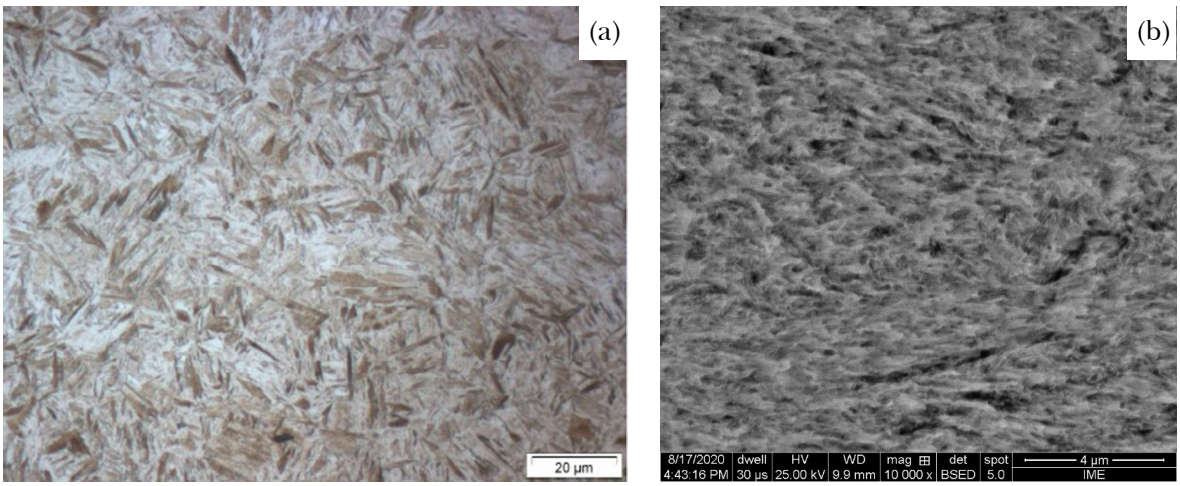

For some researchers, such as Burdekin and Folch [29], the DBTT is defined as the temperature range over which the change in energy levels from low to high occurs. However, as in practice there is usually no sudden change in energy, but rather a transition zone, it is difficult to determine the DBTT precisely. Therefore, a series of tests were carried out at different temperatures combined with macroscopic, microscopic and chemical composition analyses, which allowed the DBTT to be determined, which is an important parameter when selecting a material from the point of view of toughness or tendency to occur brittle fracture [29].

3.1 Absorbed energy

Table 3 shows the values obtained in the Charpy tests using the specimens made from the material under study. It should be noted that all the specimens separated completely during the test.

Table 3 - Charpy impact test results (values in Joule).

Temperature (°C)	CP01	CP02	CP03	Average
20.8	16.0	16.0	16.0	16.0
0.0	15.0	15.0	15.0	15.0
-20.0	15.0	14.0	14.0	14.3
-40.0	10.0	10.0	12.0	10.7
-60.0	10.0	9.0	12.0	10.3

Fig. 3 shows the absorbed energy curve as a function of temperature for the UHH-Q&T steel under study. The behavior of the curve obtained is characteristic of high-strength steels, with a relatively small variation in absorbed energy over a temperature range of -80 to 100°C [5]. It is plausible to see in the curve that at higher temperatures, the impact energy is greater and is compatible with a ductile mode of fracture. As the temperature decreases, the impact energy reduces over a relatively small temperature interval (around 20°C), from which the impact energy presents a low and essentially constant value; in this interval, the fracture mode is brittle.

The absorbed energy value is obtained by directly reading the value on the tester's scale. By plotting these values as a function of the temperature used in the test, it is possible to verify the change in the material's behavior according to the change in temperature. The plateau regions were identified by visual examination of the points plotted on the graph. Thus, it was found that the lower plateau comes at a temperature of -60°C, while the upper plateau comes in the range of 0°C to 20.8°C.

After defining the energy thresholds, the transition region (-40 to -20°C) was adjusted by linear regression. The results are shown in **Fig. 4**. Next, the hyperbolic tangent was adjusted using the MS – Excel Solver function. **Fig. 5** shows the results obtained: the graphical form; the equation of the adjusted hyperbola; and the value of the correlation coefficient (R^2) relating to the adjustment of the experimental points with the hyperbolic tangent curve.

Fig. 3 - Absorbed energy curve as a function of temperature in the Charpy impact test.

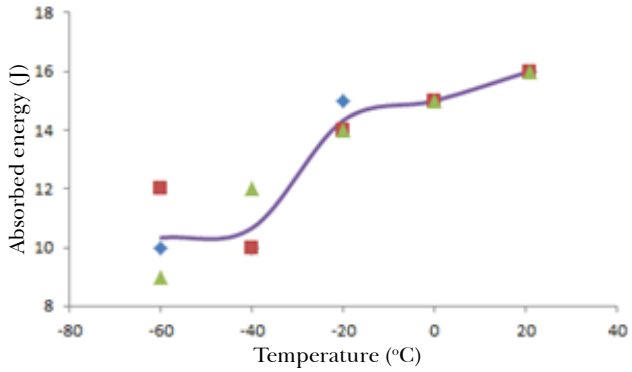

Fig. 4 - Linear regression of the transition region.

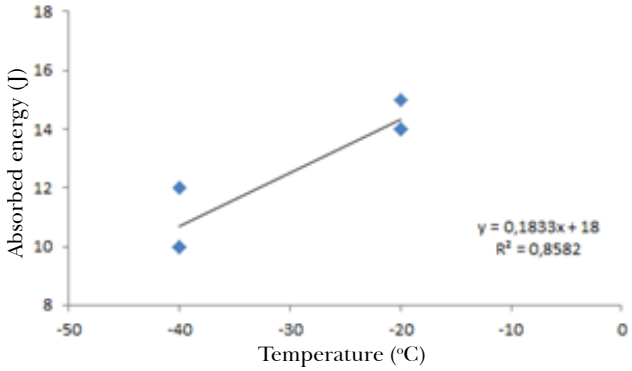

Fig. 5 - Absorbed energy curve as a function of temperature adjusted by the hyperbolic tangent method.

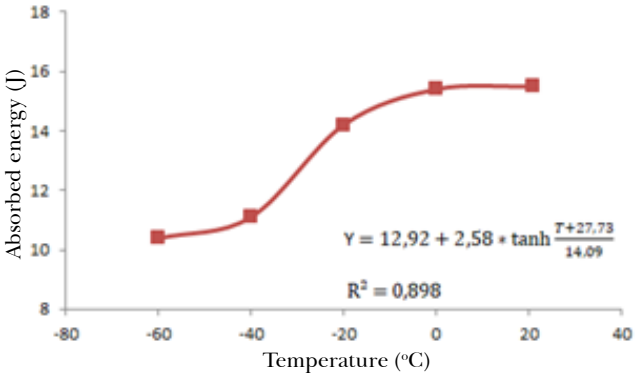

By drawing up the graphs shown, it was possible to determine the following parameters, which are illustrated **in Fig. 6**: temperatures $DBTT_{EA}$, $DBTT_{BN}$ and

$DBTT_{(ND)}$; and energy of the upper parameter (EUP) and lower parameter (ELP). **Table 4** shows the values of these parameters and the temperatures of the upper parameter (TUP) and lower parameter (TLP) by absorbed energy criterion.

Fig. 6 - Parameters $DBTT_{EA}$, $DBTT_{BN}$, $DBTT_{(ND)}$), EUP and ELP.

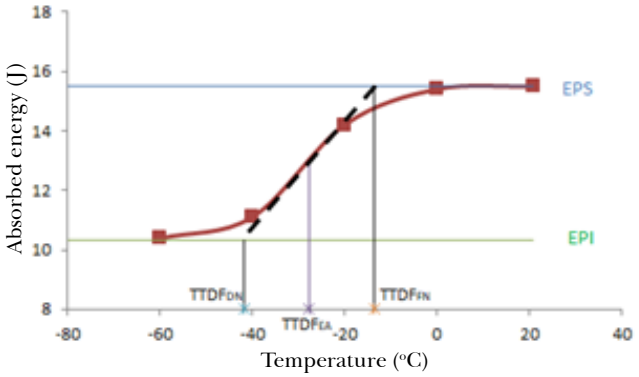

Table 4 - Results obtained by absorbed energy criterion using the hyperbolic tangent method.

Parameter	Value
$DBTT_{(EA)}$ (°C)	-27.73
$DBTT_{(BN)}$ (°C)	-41.83
$DBTT_{(ND)}$ (°C)	-13.64
EUP (J)	15.50
TUP (°C)	-13.64
ELP (J)	10.33
TLP (°C)	-41.83

3.2 Macroscopic and microscopic analysis

The macrographs of the fracture surfaces of the specimens are shown in **Fig. 7**. It is visually noticeable that, although there is a likelihood of a discrepancy occurring, as the test temperature decreases, there is a decrease in shear fracture, i.e. the percentage of ductile fracture area decreases, giving way to brittle fracture. With regard to the topic of lateral expansion, there was no evidence of this occurring, even in specimens at 0°C and room temperature, classified at first as mainly ductile.

It is possible to classify and quantify these fractures by means of qualitative and quantitative analyses of the percentage of ductile fracture, respectively, using the ASTM E23 standard as a reference [16]. However, other studies [30-31] have shown that the values obtained when each of the different definitions for determining DBTT is adopted are different from each other. As a result, measuring DBTT values based on qualitative and

quantitative ductile fracture percentage criteria, despite also being results of the evaluation of the fracture faces of the test specimens, are certainly susceptible to incredulity.

Table 5 shows the percentages obtained by both criteria (qualitative and quantitative) and confirms the significant differences between them. Also, when the values for the percentage of ductile fracture of the surfaces are compared with the values obtained using the absorbed energy criterion, incompatibility is observed, despite the fact that they are achieved by different criteria. From the evaluation of the fracture faces, it is clear that there is a risk of disparity between the results, since the appearance of the fracture faces of different materials can be similar.

Fig. 7 - Macroscopy of the fracture face of Charpy impact test specimens at temperatures: (a) ambient; (b) 0°C; (c) -20°C; (d) -40°C; (e) -60°C (5X magnification).

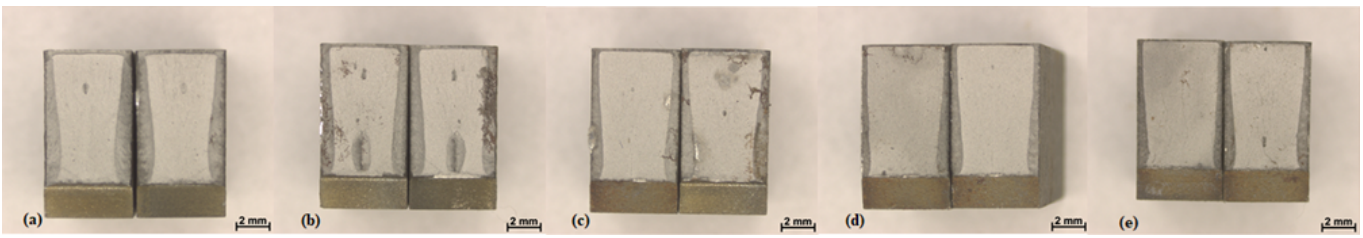

Table 5 - Percentage of ductile fracture using the ASTM E23 standard as a reference.

Temperature (°C)	% Qualitative	% Quantitative
Room	50.00	34.73
0.0	50.00	32.21
-20.0	40.00	26.28
-40.0	40.00	25.29
-60.0	20.00	9.68

Therefore, in order to study the fracture micromechanism in greater detail and obtain greater reliability, microscopic analyses of the fracture faces were conducted via SEM. The aim of this analysis was to confirm the fracture micromechanism observed through macroscopy on the fracture faces of the specimens tested under Charpy impact at the different temperatures.

The SEM micrographs of the fracture surfaces of the specimens after the tests, carried out at room temperature, -20°C and -60°C, are shown in **Fig. 8** to **Fig. 10**, respectively. The figures show the surfaces subdivided into three regions of the specimens (top, middle and bottom), noting that in the left column the magnification is 30X or 50X and in the right column the magnification is 1000X or 2000X.

It is noticeable in **Fig. 8** that the surface contains a typical feature of a predominantly ductile fracture—roughness. Another characteristic of a highly ductile fracture, dimples, are also evident on the surface. These micromechanisms are supported by the curve of absorbed energy as a function of temperature adjusted by the hyperbolic tangent method, as this would show a mainly ductile fracture.

The specimens tested at -20°C are the ones with a temperature closest to $DBTT_{EA}$ and whose fracture faces were considered mixed (as having brittle and ductile fractures), which is in line with the behavior expected of the material at the transition temperature. As shown in **Fig. 9**, where both cleavage fracture and shear fracture were considered to be present.

Fig. 10 shows micrographs of the fracture surface of the specimens after testing at -60°C. The surface characteristics show a predominant fracture resulting from the cleavage micro-mechanism, which is consistent with the region of this temperature in the curve of absorbed energy as a function of temperature adjusted by the hyperbolic tangent method.

3.3 Effect of chemical composition

A comparative analysis between the material under study and another type of tempered and quenched steel, the AISI 4340 steel studied elsewhere [32], and corroborated the prescribed effect of chemical composition on the impact fracture energy curve. In other studies, this effect is also consistent with the behavior of other steels [33]. The DBTT of AISI 4340 steel occurred at 0°C determined at 21.0 J. Its Mn, C, P and S content in % weight is 0.72, 0.42, 0.015 and 0.008, respectively [32]. As shown in **Table 1**, UHH-Q&T has a higher Mn content, inducing a rise in absorbed energy, but the higher C content encourages greater vigor instead. Therefore, partly due to this relationship, the absorbed energy of the material under study is lower (12.92 J).

3.4 Correlation between Charpy impact and fracture toughness

Both the Charpy test and the Pellini drop-weight test are still widely applied to structural materials. ASTM has standardized both tests, as well as a number of related approaches [16, 34-35]. Although these tests lack the mathematical rigor and predictive capabilities of fracture mechanics methods, these approaches provide an excellent qualitative indication of material toughness. The advantage of these qualitative methods is that they are less expensive and easier to perform than fracture mechanics tests [16, 34].

Fig. 8 - SEM images of details of the fracture face of the specimen tested by Charpy impact at room temperature.

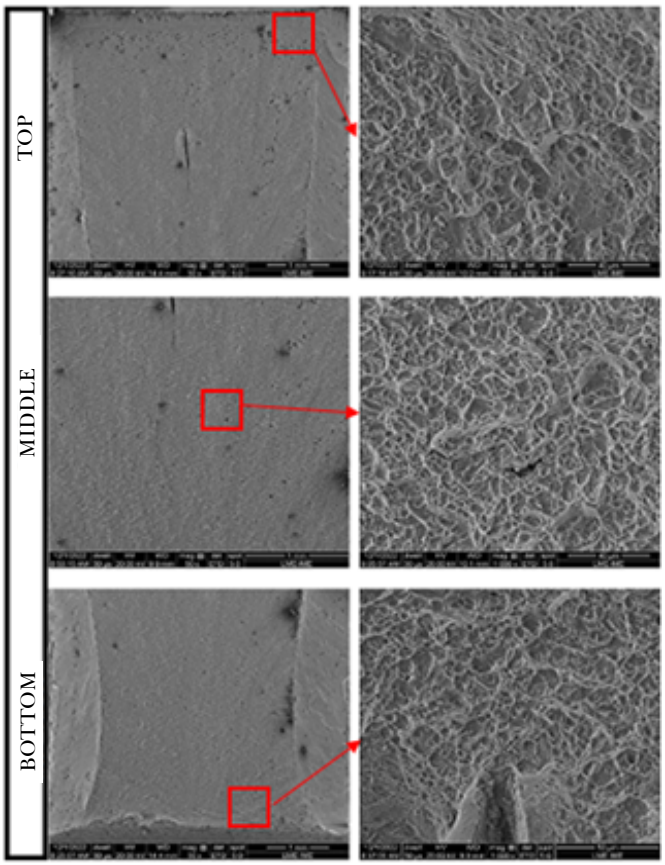

Some researchers [36-38] have correlated the absorbed energy obtained in the Charpy test with fracture toughness parameters such as K_{Ic}. Some of these empirical correlations work reasonably well, and the shipbuilding industry uses the Pellini drop-weight test to qualify steels for ship hulls. However, there are important differences between these tests and fracture mechanics tests that prevent simple relationships between qualitative and quantitative measures of toughness.

These differences include the fact that Charpy and drop-weight test specimens have an initial notch, while fracture mechanics specimens have significant fatigue cracks [16, 34].

When the material available does not allow Charpy impact specimens to be made to the standard size (10 x 10 x 55 mm), smaller ones can be used, as was the case in this study, but the results obtained with different specimen sizes cannot be compared directly. When Charpy specimens with dimensions smaller than the standard, i.e. sub-size, are required or specified, they can be selected in accordance with Annex *A3–Additional Impact Test Specimen Configurations* of the ASTM E23 standard [16].

Fig. 9 - SEM images of details of the fracture face of the specimen tested by Charpy impact at -20°C.

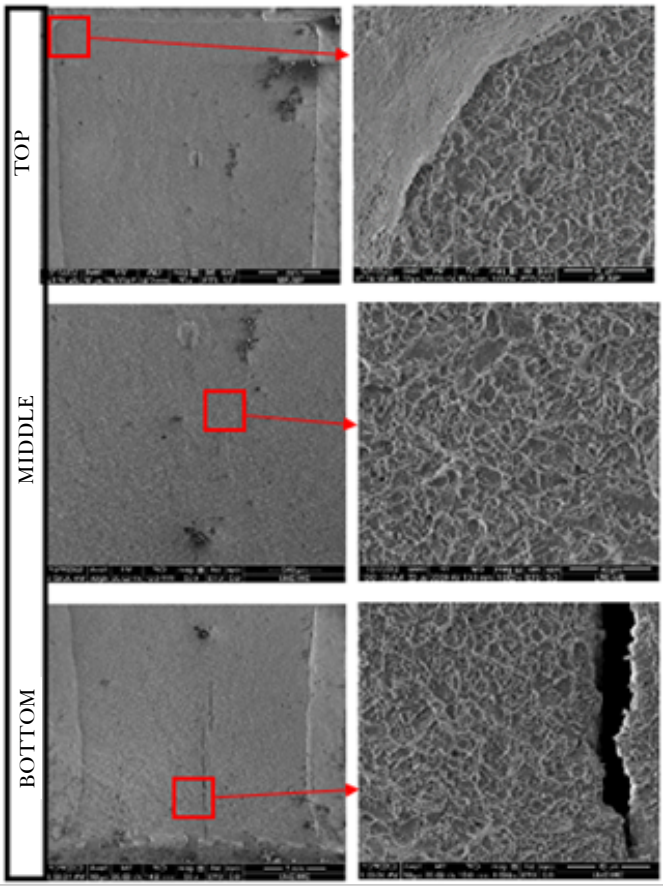

Varying, increasing or decreasing the thickness and/or width of the specimen tends to modulate the volume of the metal subjected to distortion and, as a result, also tends to change the energy absorbed.

However, any increase in size, particularly in thickness, also tends to increase the degree of restriction and, by tending to induce brittle fracture, can decrease the energy absorbed [16].

Fig. 10 - SEM images of details of the fracture face of the specimen tested by Charpy impact at -60°C.

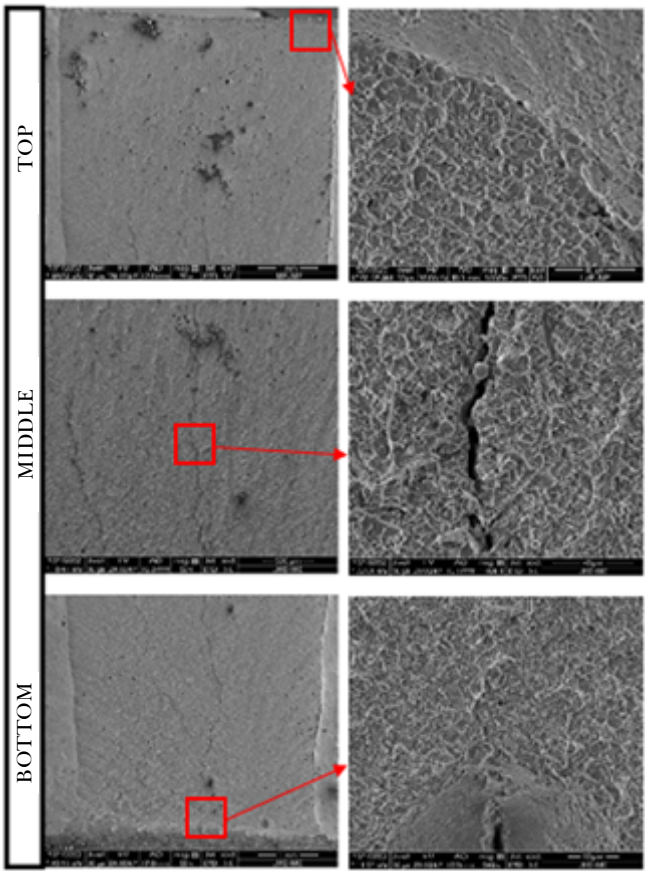

A general correlation between the absorbed energy values obtained with specimens of different sizes or shapes is not feasible, but limited correlations can be established for specification purposes based on special studies of specific materials and specimens [16].

4. Conclusions

From the methodology used in the Charpy impact test combined with fractographic analysis, it was possible to obtain a better understanding of impact tests and material behavior analysis, thus enabling the verification of energy absorbed as a function of temperature for specimens tested at different temperatures. It can be said that this is the most appropriate method for determining the DBTT of UHH-Q&T steel.

The tests showed that it is possible to obtain mechanical properties in terms of the toughness of a material by means of impact. Through this development, it was realized that temperature influences the toughness of the material, obtaining, for the specimen tested, a predominantly brittle structure at low temperatures and a dominant ductile structure at room temperature, certified by micrography. In this way, the correct material to use at different temperatures can be determined.

By evaluating the fracture faces of the specimens by SEM, it was possible to see that in the specimens tested in the transition zone there are regions where, by visual evaluation, it was considered that there was cleavage fracture, but in these there are also regions with alveoli resulting from plastic deformation of the material, typical of ductile fracture. The qualitative and quantitative criteria are therefore doubtful.

The results show that the DBTT based on 12.92 J of absorbed energy is -27.73°C. In addition, the temperature at which the zero ductility transition occurs is -41.83°C and the zero brittleness transition occurs at -13.64°C.

Acknowledgements

The authors would like to thank SSAB Special Steels for supplying the base material, the Mechanical Testing and Scanning Electron Microscopy Laboratories of the Materials Engineering Section of the Instituto Militar de Engenharia (IME) and the Materials Characterization Laboratory (LACAM) of the Universidade Federal do Pará (UFPA) for providing testing and microstructural characterization facilities for this work.

References

[1] U.S. **Military Specification, MIL-DTL-46100E (MR). Armor Plate, Steel, Wrought, High-Hardness**. U.S. Army Research Laboratory, APG, MD, 9 July 2008.

[2] RAPACKI, E.; FRANK, K.; LEAVY, B.; KEELE, M.; PRIFTI, J. **Armor** steel hardness influence on kinetic energy penetration proceedings. In: INTERNATIONAL SYMPOSIUM ON BALLISTICS, 15., Jerusalem, 1995.

[3] SSAB. Armor: The steel you want between you and risk. Sweden: SSAB, 2017.
[4] BACKMAN, M. E.; GOLDSMITH, W. The mechanics of penetration of projectiles into targets. **International Journal of Engineering Science**, [s. l.], v. 16, p. 1-99. 1978.
[5] PEREIRA, L. C., BLAS, J. C. G., GRIZA, S., DARWISH, F. A. I. Use of instrumented Charpy testing on the fracture toughness characterization of metallic materials. **Tecnologia em Metalurgia, Materiais e Mineração**, [s. l.], v. 18, p. 1-11. 2021.
[6] TANAKA, M.; UMEKAWA, S. On the breaking behaviour in Charpy impact bending tests. In: JAPAN CONGRESS FOR TESTING MATERIALS, 1., Kyoto, 1958.
[7] ONO, S. Micro-time structure of impact fracture concerning Charpy test. In: JAPAN CONGRESS FOR TESTING MATERIALS, 1., Kyoto, 1958.
[8] TAGAWA, T.; KAYAMORI, Y.; HIRA, H. Statistical scatter of fracture toughness in the ductile–brittle transition of a structural steel. **Eng. Fract. Mech**., v. 77, n. 16, p. 3077-3086, 2010.
[9] CHEN, S. L.; HU, J.; ZHANG, X. D. et al. High ductility and toughness of a micro-duplex medium-Mn steel in a large temperature range from -196°C to 200°C. **Journal of Iron and Steel Research International**, [s. l.], v. 22, p. 1126-1130, 2015.
[10] GOPALAN, A.; SAMAL, M. K.; CHAKRAVARTTY, J. K. Fracture toughness evaluation of 20MnMoNi55 pressure vessel steel in the ductile to brittle transition regime: Experiment & numerical simulations. **J. Nucl. Mater**., [s. l.], v. 465, p. 424-432, 2015.
[11] CHAO, Y. J.; WARD, J. D.; SANDS, R. G. Charpy impact energy, fracture toughness and ductile–brittle transition temperature of dual-phase 590 steel. **Mater. Design**, [s. l.], v. 28, p. 551-557, 2007.
[12] TANGUY, B.; BESSON, J.; PIQUES, R.; PINEAU, A. Ductile to brittle transition of an A508 steel characterized by Charpy impact test: Part I: Experimental results. **Eng. Fract. Mech**., [s. l.], v. 72, p. 49-72, 2005.
[13] HAUŠILD, P.; NEDBAL, I.; BERDIN, C.; PRIOUL, C. The influence of ductile tearing on fracture energy in the ductile-to-brittle transition temperature range. **Materials Science and Engineering: A**, [s. l.], v. 335, p. 164-174, 2002.
[14] ROSENFIELD, A. R.; SHETTY, D. K.; SKIDMORE, A. J. Fractographic observations of cleavage initiation in the ductile-brittle transition region of a reactor-pressure-vessel steel. **Metallurgical Transactions A**, v. 14, p. 1934-1937, 1983.
[15] TAKASHIMA, Y.; MINAMI, F. Prediction of Charpy absorbed energy of steel for welded structure in ductile--to-brittle fracture transition temperature range. **Quarterly Journal of the Japan Welding Society**, v. 38, p. 103-107, 2020.
[16] AMERICAN SOCIETY FOR TESTING AND MATERIALS. **ASTM E23**: Standard test methods for notched bar impact testing of metallic materials. U.S.: American Society for Testing and Materials, 2018.
[17] ZHANG, X.; QU, Y.; LI, R. Low temperature impact toughness and fracture analysis of EN-GJS-400-18-LT ductile iron under instrumented impact load. **Journal of Iron and Steel Research International**, [s. l.], v. 22, p. 864-869, 2015.
[18] SAMAL, M. K.; CHAKRAVARTTY, J. K.; SEIDENFUSS, M.; ROOS, E. Evaluation of fracture toughness and its scatter in the DBTT region of different types of pressure vessel steels. **Engineering Failure Analysis**, v. 18, p. 172-185, 2011.
[19] DIETER, G. E. **Mechanical Metallurgy**. 2. ed. New York: McGraw-Hill Book Company, 1981.
[20] LEACH, P. W.; WOODWARD, R. L. The influence of microstructural anisotropy on the mode of plate failure during projectile impact. **J. Mat. Sci**., [s. l.], v. 20, p. 854-858, 1985.
[21] MANGANELLO, S. J.; ABBOTT, K. H. Metallurgical factors affecting the ballistic behaviour of steel targets. **J. Mat**., [s. l.], v. 7, p. 231-239, 1972.
[22] SHOWALTER, D. D. et al. STANDARD, Australian Defence. DEF (AUST) 8030. Rolled Armour Plate, Steel (3-35 mm). **Army Research Laboratory,** Adelphi, 2005.
[23] HERZIG, N ; MEYER, L. W.; PURSCHE, F., HUSING, K. Relation between dynamic strength and toughness properties and the behavior under blast conditions of high strength steels. In: INTERNATIONAL SYMPOSIUM ON IMPACT ENGINEERING, 7., 2010. **Anais** […]. Warsaw: MABS, 2010. p. 278-284.
[24] BRITISH STANDARD. BS EN 10029: Hot-rolled steel plates 3 mm thick or above – tolerances on dimensions and shape. UK: British Standard, 2010.
[25] BRITISH STANDARD. **BS EN 10163-2**: Delivery requirements for surface condition of hot-rolled steel plates, wide flats and sections — Part 2: Plate and wide flats. UK: British Standard, 2004.

[26] SSAB. **General product information strenx, hardox, armox and toolbox – UK**. [s. l.]: SSAB, 2018.
[27] ERICKSONKIRK, M.; SHAIKH, A.; ERICKSONKIRK, M. Insights and observations arising from curve-fitting the Charpy V-notch and tensile data contained within the United States' light water reactor surveillance database. ASME 2008 PRESSURE VESSELS AND PIPING CONFERENCE. 2008. Chicago, 2008. p. 389-396.
[28] AMERICAN SOCIETY FOR TESTING AND MATERIALS. **ASTM E2142**: Standard test methods for rating and classifying inclusions in steel using the scanning electron microscope. West Conshohocken: American Society for Testing and Materials, 2015.
[29] FOLCH, L.; BURDEKIN, F. M. Application of coupled brittle-ductile model to study correlation between Charpy energy and fracture toughness values. **Eng. Fract. Mech**., [s. l.], v. 63, p. 57-80, 1999.
[30] ZHAO, Y. J.; SU, Y. M.; LIU, M.; HU, Z. L.; TANG, P. Ductile-to-brittle transition and impact fracture behavior of 3Mn–Si–Ni low carbon martensitic steel. **Strength of Materials**, [s. l.], v. 51, p. 291-299, 2019.
[31] TAKASHIMA, Y.; ITO, Y.; LU, F.; MINAMI, F. Fracture toughness evaluation for dissimilar steel joints by Charpy impact test. **Welding in the World**, [s. l.], v. 63, p. 1243-1254, 2019.
[32] DUARTE, A. S. **Metodologia básica para a produção de materiais de referência para a calibração indireta de máquinas pendulares de impacto Charpy**. 2006. Dissertação (Mestrado em Engenharia de Materiais) – Universidade Federal de Ouro Preto, Ouro Preto, 2006.
[33] ROE, G. J.; BRAMFITT, B. L. **Notch toughness of steels. ASM International, Metals Handbook**. Materials Park: ASM Handbook, 1990.
[34] AMERICAN SOCIETY FOR TESTING AND MATERIALS. **ASTM E208**: Standard test method for conducting drop-weight test to determine nil-ductility transition temperature of ferritic steels. West Conshohocken: American Society for Testing and Materials, 2020.
[35] AMERICAN SOCIETY FOR TESTING AND MATERIALS. **ASTM E436-03**: Standard test method for drop-weight tear tests of ferritic steels. West Conshohocken: American Society for Testing and Materials, 2021.
[36] TEERI, T.; KUOKKALA, V.-T.; SIITONEN, P.; KIVIKYTÖ-REPONEN, P.; LIIMATAINEN, J. Impact wear in mineral crushing. **Proceedings of the Estonian Academy of Sciences Engineering**, [s. l.], v. 12, p. 408-418, 2006.
[37] ZAMBRANO, O. A. A review on the effect of impact toughness and fracture toughness on impact-abrasion wear. **Journal of Materials Engineering and Performance**, Materials Park, v. 30, p. 7101-7116, 2021.
[38] WALLIN, K. A simple theoretical Charpy-V-K correlation for irradiation embrittlement. In: MARRIOT, D. L.; MAGER, T. R.; BAMFORD, W. H. (Eds.). **Innovative Approaches to Irradiation Damage and Fracture Analysis**. v. 170. New York: ASME – American Society of Mechanical Engineers, 1989. p. 93-100.